

SPARSE ARRAY TOMOGRAPHY SYSTEM FOR CORROSION EXTENT MONITORING

H. Bian, H. Gao, J. Rose

Pennsylvania State University, University Park, PA, USA

Abstract: A sparse array guided wave tomography system is investigated for monitoring plate wall thinning status caused by corrosion/erosion. Because of their group velocity dependence on the structure wall thickness of some special modes, ultrasonic guided waves are sensitive to structure wall thinning status. As a low resolution imaging technique, a sparse array system provides many advantages. First, the data collection procedure is not as tedious as other tomography systems because of its low data amount requirement; second, in a sparse array case, direct matrix inversion techniques are feasible for tomographic reconstruction which leads to a fast reconstruction procedure; in addition, this system is robust in a sense that it is less sensitive to signal noise contamination. Therefore, this technique provides a practical solution for real time monitoring of industrial structures.

Several guided wave features are extracted for image reconstruction including for example wave attenuation coefficient, refractive index or group velocity, and signal frequency shift. Results show that all of these features have the potential of providing useful information about structural integrity, while the frequency shift feature is more stable in the context of noise contamination and is also less dependent on the guided mode selection in our case.

Introduction: Tomography is a cross-sectional imaging reconstruction technique via collecting energy data along the perimeter of an object in a regular pattern. Beyond the revolutionary impact of X-ray CT on diagnostic medicine, the CT technique has been successfully extended to many other fields, such as geophysics, space science, nondestructive evaluation (NDE), and industrial process control, with multiple energy source choices, from X-ray, radioisotopes, and magnetic resonance, to ultrasound and microwave. With the development of new algorithms and the high calculation speed of modern computers, now CT technique can provide us real-time 2D/3D images with high accuracy [1].

Ultrasonic guided waves can propagate along many natural wave-guides, such as ship hulls, airline shells and pipelines. Guided waves can travel long distances along wave-guides without apparent attenuation, and provide structural integrity information for all points along its wave path, instead of point by point as in the case of conventional ultrasonic C-scan [2]. In addition, ultrasonic guided modes are waves that are sensitive to structural anomalies such as wall thinning, cracks, and other mechanical changes. Consequently, ultrasonic guided waves have the advantage of providing faster, cost efficient and labor efficient solutions for structural health monitoring. Guided wave technology has attracted the attention of researchers in the field of nondestructive evaluation (NDE) for decades, and has become a standard technique in evaluating the integrity of structures that can be considered as natural waveguides, especially shells, plates, and pipe-like structures.

Ultrasonic guided wave computerized tomography (GWCT) is a new and promising technology, and combines all the merits of guided waves and CT [3-10]. One area where guided wave CT can offer an ideal solution is to map plate wall thinning caused by corrosion/erosion, which nowadays is a big concern in many industries. This new guided wave CT technology is based on the group velocity dependence on the structure wall thickness of some special guided

modes, offering a reliable index for corrosion/erosion degree. Properly selecting guided modes and a frequency range is the key for success. As the technique manipulation is concerned, a sparse transducer array is applied and correspondingly direct matrix inversion techniques are applied to reconstruct the tomograms. By applying a reduced number of transducers, GWCT imaging could be real time with reasonable image quality.

Results: Guided wave mode selection depends on the guided wave group velocity dispersion feature. Figure 1 shows Lamb wave group velocity dispersion curves of aluminum plates. With an aluminum specimen thickness of 1/8 inch, two frequencies are selected for the experiments which are 0.39 MHz and 0.49 MHz, and hence the product of frequency and plate thickness are, respectively, 1.24 MHz*mm and 1.56 MHz*mm. When the S0 Lamb mode is applied, these two excitation points correspond to the area where the group velocity is sensitive to plate thickness variation according to the dispersion curves shown in figure 1. Experimental specimen geometry and the wall thinning status which is designed to capture the gradual corrosion/erosion feature in a real situation are depicted in figure 2. Also shown in figure 2 is the position of the circular transducer array which consists of equally spaced 8 circular PZT crystals with central frequency around 0.4MHz and radius 1/4 inch.

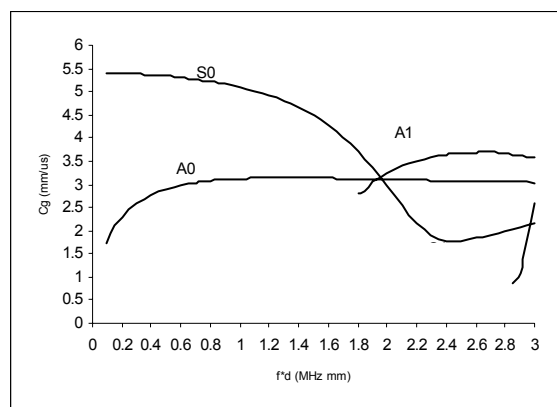


Figure 1 Lamb wave group velocity dispersion curves of aluminum plates.

A-scan waveforms are collected for every possible wave path which is of 28 pieces for an 8 transducer system. Straight ray paths are assumed and no wave diffraction effect is taken into account. Several features are extracted from the ultrasound waveforms including amplitude, time of flight (TOF) and frequency shift of the signals which are later on used for obtaining tomograms. With limited signal information, direct matrix reconstruction techniques are feasible in this case and are exploited for tomography image reconstruction. This image reconstruction approach makes the reconstruction much faster compared with transformed based and iterative reconstruction algorithms.

Some results are presented in the following. Figures 3, 4, and 5 are, respectively, tomograms of refractive index (reciprocal of velocity), attenuation coefficient and frequency shift reconstructed from signals with central frequency of 0.39 MHz; while figures 6, 7, and 8 are, respectively, tomograms of refractive index (reciprocal of velocity), attenuation coefficient and frequency shift reconstructed from signals with central frequency of 0.49 MHz.

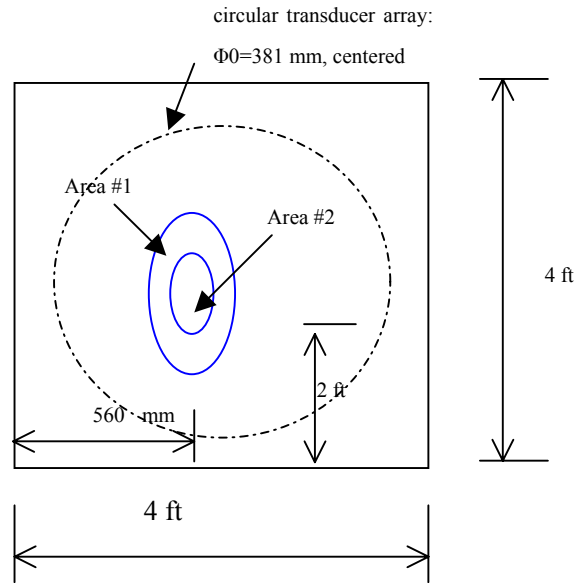


Figure 2 Experimental specimen and circular transducer array layout. Specimen thickness: 1/8 inch. Outer ellipse: $\Phi_1=200$ mm, $\Phi_2=100$ mm; inner ellipse: $\Phi_1=100$ mm, $\Phi_2=50$ mm.

Discussion: Results show that all features studied here have the potential of detecting the wall thickness variation. Frequency shift information provides the best estimation of the real structure situation and is less dependent on the mode selected, which is clear from the high similarity of figure 5 and figure 8. The attenuation coefficient is a good signature too, although it is sensitive to the coupling situation between transducers and the specimen. Ultrasound refractive index, which is theoretically sensitive to wall thickness changing, even if suffering dispersion while passing through the specimen at our working range, is still a good feature to provide pseudo-image of the structure corrosion/erosion extent.

Concluding Remarks: Although only 8 transducers are exploited and 28 pieces of signals are collected, the tomographic results show great potential of guided wave tomography as sensitive index of structure wall thinning with advantages of efficient data collection and fast tomogram reconstruction.

Several signal features can be selected for tomographic reconstruction. Among them, the frequency shift is less dependent on the guided mode selection in our study. By properly selecting guided mode and data collection configuration, guided wave CT could be a useful tool for real time structure wall thickness mapping in corrosion/erosion detection of many industries.

Acknowledgments: This material is based on work of the project “Guided Wave Tuning for Enhanced Tomographic Imaging” supported by 2003 ASNT fellowship. Thanks also to Intelligent Automation, Rockville, MD for partial support of the work.

Special thanks go to Dr. M. K. Hinders and his group at College of William and Mary for early training on the subject of ultrasonic tomography.

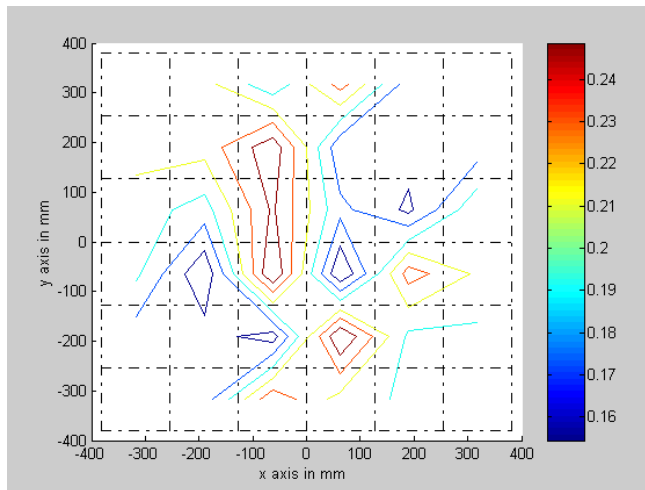


Figure 3 A tomogram of refractive index with signal central frequency 0.39 MHz.

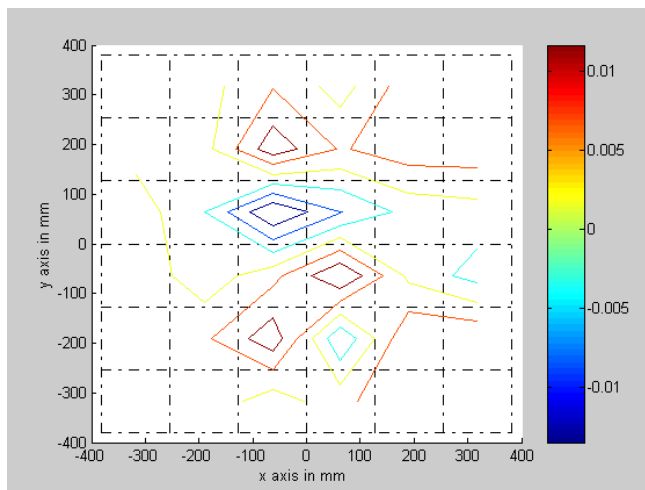


Figure 4 A tomogram of attenuation coefficient with signal central frequency 0.39 MHz.

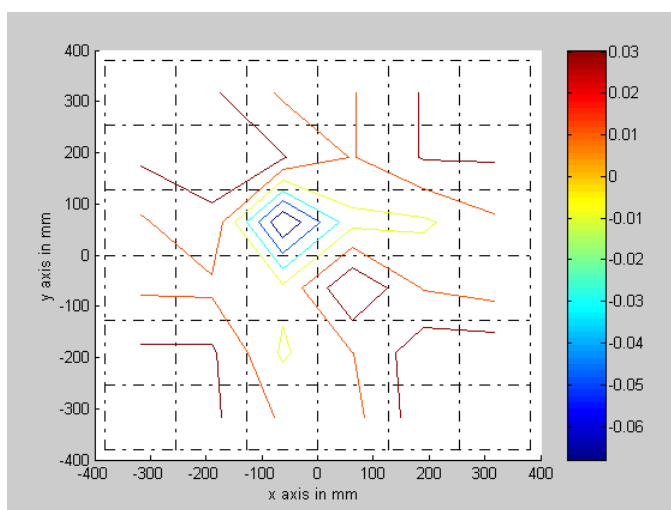


Figure 5 A tomogram of frequency shift with signal central frequency 0.39 MHz.

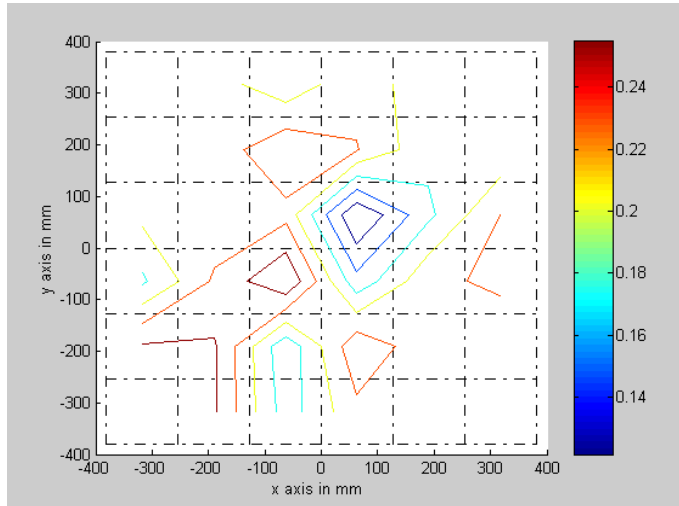


Figure 6 A tomogram of refractive index with signal central frequency 0.49 MHz.

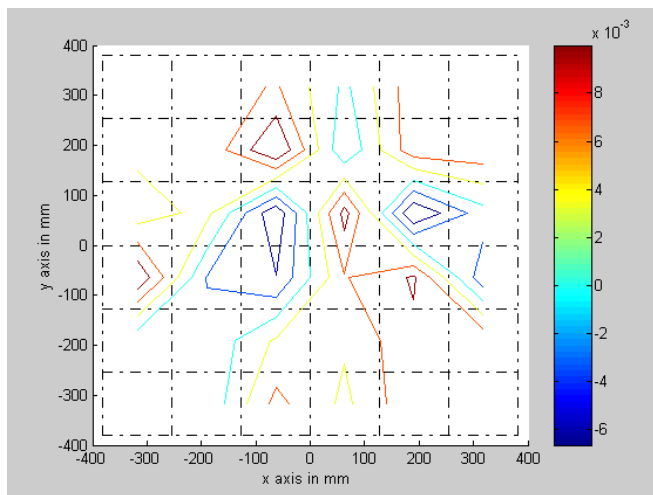


Figure 7 A tomogram of attenuation coefficient with signal central frequency 0.49 MHz.

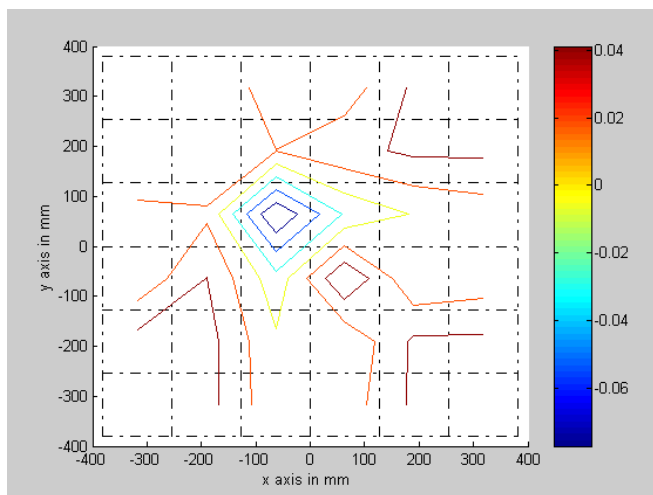


Figure 8 A tomogram of frequency shift with signal central frequency 0.49 MHz.

References:

1. Avinash C. Kak, Malcolm Slaney, *Principles of Computerized Tomographic Images*, IEEE press, 1988.
2. Rose, J.L., *Ultrasonic Waves in Solid Media*, Cambridge Press, 1999.
3. L. Capeneri, H. G. Tattersall, J. A. G. Temple, and M. G. Silk. "Time-of-flight Diffraction Tomography for NDT Applications." *Ultrasonics*, **30**, No 5, 1992.
4. D. P. Jansen, D. A. Hutchins, and J. T. Mottmam. "Lamb Wave Tomography of Advanced Composite Laminates containing Damage." *Ultrasonics*. **32**, No 2, 1994.
5. D. A. Hutchins, D. P. Jansen, and C. Edwards. "Lamb-wave Tomography using Non-contact Transduction." *Ultrasonics*. **31**, No. 2, 1993.
6. D. P. Jansen and D. A. Hutchins. "Immersion Tomography using Rayleigh and Lamb Waves." *Ultrasonics*. **30**, No. 4, 1992.
7. J. C. P. McKeon, M. K. Hinders, "Parallel Projection and Crosshole Lamb Wave Contact Scanning Tomography," *JASA*, **106(5)**, Nov. 1999, p2568-2577.
8. E. V. Malyarenko, M. K. Hinders, "Fan Beam and Double Crosshole Lamb Wave Tomography for Mapping Flaws in Aging Aircraft Structures," *JASA*, **108(4)**, Oct. 2002, p1631-1639.
9. J. C. P. McKeon, M. K. Hinders, "Lamb Wave Scattering form a Through Hole," *Journal of Sound and Vibration*, **224(5)**, Nov. 1999, p843-862.
10. E. V. Malyarenko, M. K. Hinders, "Ultrasonic Lamb Wave Diffraction Tomography," *Ultrasonics*, **39**, 2001, p269-281.